



# Triple-Responsive Polyampholytic Graft Copolymers as Smart Sensors with Varying Output

Johannes B. Max, Afshin Nabiyan, Jonas Eichhorn, and Felix H. Schacher\*

Three triggers result in two measurable outputs from polymeric sensors: multiresponsive polyampholytic graft copolymers respond to pH-value and temperature, as well as the type and concentration of metal cations and therefore, allow the transformation of external triggers into simply measurable outputs (cloud point temperature ( $T_{CP}$ ) and surface plasmon resonance (SPR) of encapsulated silver nanoparticles). The synthesis relies on poly(dehydroalanine) (PDha) as the reactive backbone and gives straightforward access to materials with tunable composition and output. In particular, a rather high sensitivity toward the presence of  $Cu^{2+}$ ,  $Co^{2+}$ , and  $Pb^{2+}$  metal cations is found.

From health and environmental perspectives, heavy metal sensing is of special interest for quantitative and qualitative analyses of aqueous systems.<sup>[1]</sup> Among others, promising materials for corresponding sensors are smart polymers, which can translate external stimuli such as light, temperature, pH, or the presence of metal ions into a physical or chemical readout.<sup>[2–4]</sup> If such materials contain specific binding sites for different metal ions, the optical properties such as absorbance, fluorescence, and luminescence<sup>[5–9]</sup> or the solution behavior, e.g., the lower critical solution temperature (LCST)<sup>[10,11]</sup> or simply the hydrodynamic size,<sup>[12]</sup> of a responsive polymer will significantly change upon metal chelation. Hereby, recent progress in the polymerization of functional monomers allows us to incorporate strong ligands such as bipyridine units,<sup>[9]</sup> crown ethers,<sup>[10]</sup> carboxylates, or imidazoles.<sup>[11]</sup> However, as recently shown for materials featuring both carboxylate and hydroxyl moieties, complexation also

strongly depends on coordination behavior and concentration of the respective metal ion, affecting inter- and intramolecular interactions within polymer chains.<sup>[13,14]</sup>

Polyelectrolytes exhibit ionizable groups in each repeat unit<sup>[15]</sup> and, therefore, are an interesting polymer class for metal ion sensing,<sup>[16,17]</sup> but also for separation and flocculation processes,<sup>[18,19]</sup> catalysis,<sup>[20]</sup> or as antimicrobially active materials.<sup>[21]</sup> Further tuning of material properties can be achieved by combining ionic and hydrophobic monomers,<sup>[22]</sup> different polymerization techniques,<sup>[23,24]</sup> or postpo-

lymerization modification reactions. Of particular interest are examples, which maintain solubility in water even after metal complexation, as shown for double hydrophilic co-polyelectrolytes<sup>[13,14,25]</sup> or multistimuli-responsive copolymers.<sup>[26,27]</sup> Going even further, the combination of different stimuli within one material opens up a wide space of sensing applications, as shown for chitosan-g-poly(*N*-isopropylacrylamide) (PNIPAAm) graft copolymers featuring a pH-responsive polyelectrolyte backbone and thermoresponsive side chains.<sup>[27]</sup>

Poly(dehydroalanine) (PDha), a polyampholyte featuring high charge density and both amine and carboxylate moieties in every repeat unit,<sup>[28]</sup> was introduced recently as a versatile platform to obtain tailor-made copolymers with defined hydrophilicity,<sup>[29,30]</sup> as a building block in double hydrophilic block copolymers,<sup>[31]</sup> or as a template for the pH-controlled formation of Au/Ag alloy nanoparticles.<sup>[32]</sup> Hereby, the polyampholytic PDha backbone offers pH-dependent net charge and a high density of functional groups as anchoring points for grafts or as binding sites for metal ions.<sup>[31,32]</sup> We now introduce thermoresponsive PDha-based graft copolymers by grafting one single NIPAAm unit. While PNIPAAm is probably the most studied LCST polymer overall,<sup>[33]</sup> this effect has so far not been shown for short side chains. However, high NIPAAm contents (>90 mol%) in poly(*N*-isopropylacrylamide-*co*-maleic acid-*co*-1-vinylimidazole) terpolymers were shown to be of interest for metal ion recognition.<sup>[11]</sup> In our case, we combine thermoresponsive of NIPAAm grafts with pH-dependent charge and metal ion complexation of the PDha backbone, resulting in triple-responsive graft copolymers. These materials are highly sensitive sensors, where even the output can be tuned.

We have shown recently that grafting different side chains to PDha backbones allows us to tune solubility and surface affinity.<sup>[30,32]</sup> We now performed aza-Michael additions under basic aqueous conditions to attach NIPAAm side chains and, with that, create triple-responsive graft copolymers (**Scheme 1**). PDha with an apparent molecular weight of  $M_n = 10\,000\text{ g mol}^{-1}$  was used,<sup>[32]</sup> and successful synthesis was proven *via*  $^1\text{H}$ - and

J. B. Max, A. Nabiyan, J. Eichhorn, Prof. F. H. Schacher  
Institute of Organic Chemistry and Macromolecular Chemistry  
Friedrich-Schiller-Universität Jena  
Lessingstraße 8, Jena 07743, Germany  
E-mail: felix.schacher@uni-jena.de

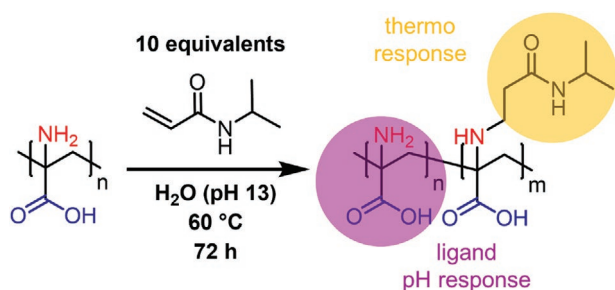
J. B. Max, A. Nabiyan, J. Eichhorn, Prof. F. H. Schacher  
Jena Center for Soft Matter (JCSM)  
Friedrich-Schiller-Universität Jena  
Philosophenweg 7, Jena 07743, Germany

J. B. Max, A. Nabiyan, J. Eichhorn, Prof. F. H. Schacher  
Center for Energy and Environmental Chemistry (CEEC)  
Friedrich-Schiller-Universität Jena  
Philosophenweg 7, Jena 07743, Germany

 The ORCID identification number(s) for the author(s) of this article can be found under <https://doi.org/10.1002/marc.202000671>.

© 2020 The Authors. Macromolecular Rapid Communications published by Wiley-VCH GmbH. This is an open access article under the terms of the Creative Commons Attribution-NonCommercial-NoDerivs License, which permits use and distribution in any medium, provided the original work is properly cited, the use is non-commercial and no modifications or adaptations are made.

DOI: 10.1002/marc.202000671



**Scheme 1.** Synthetic route toward the synthesis of a triple-responsive graft copolymer based on PDha.

$^{13}\text{C}$ -NMR spectroscopy, as well as fourier transformation infrared spectroscopy (FT-IR spectroscopy) and size exclusion chromatography (SEC) measurements (Figure S1, Supporting Information).

Kinetic investigations (Figure S2, Supporting Information) of the grafting process revealed a linear increase of the degree of functionalization (DoF) with time and a maximum of 95% grafting density upon use of 20 equivalents of the Michael acceptor. Thus, the amount of NIPAAm side chains can be precisely adjusted, and it strongly influenced the solubility of the resulting PDha-g-NIPAAm graft copolymers. Solubility in water even under acidic conditions, where PDha is typically insoluble, could be achieved starting from DoF = 30% and the dissolution in organic solvents such as methanol and *N,N*-dimethyl formamide DMF at DoF  $\geq$  50% (Table S1, Supporting Information) was possible. The  $\zeta$ -potential and titration curve (Figure S3, Supporting Information) of PDha-g-NIPAAm<sub>95</sub> (where the subscript represents the DoF) still resemble the parent ampholytic PDha homopolymer, showing pH-dependent charge through protonation/deprotonation of

carboxylic and amino groups.<sup>[32,34]</sup> By exploiting the PDha backbone as a reactive handle, also other acrylamides can be used, broadening the range of accessible graft copolymers.<sup>[35]</sup>

Since both PDha-g-NIPAAm<sub>50</sub> and PDha-g-NIPAAm<sub>95</sub> were soluble over the entire pH range, these graft copolymers were chosen for the investigation of their thermoresponsive properties (Figure 1). In comparison to PNIPAAm, monomeric NIPAAm side chains exhibit a different local environment and are, especially in case of PDha-g-NIPAAm<sub>50</sub>, also locally separated. Besides, the polyampholytic backbone exhibits pH-dependent net charge and solubility. As a result, no cloud points could be detected at pH 7 and above for PDha-g-NIPAAm<sub>50</sub>, which we ascribe to electrostatic repulsion of the negatively charged carboxylates along the PDha backbone. However, in case of PDha-g-NIPAAm<sub>95</sub> at pH 7, a cloud point temperature ( $T_{\text{CP}}$ ) of 37 °C can be observed. Upon decreasing the pH to 6, a cloud point became apparent for PDha-g-NIPAAm<sub>50</sub>, which decreases from 43 to 28 °C at pH 5 as a result of partial protonation of the carboxylic groups in accordance with potentiometric titrations (Figure S3, Supporting Information). Charge neutrality could lead to strong electrostatic attraction as a possible explanation for the lowest  $T_{\text{CP}}$  at pH 5. Further protonation of carboxylic groups enables the formation of hydrogen bonds and aggregation is facilitated. At pH 1 all carboxylic groups would be protonated and the hydrogen bonds predominate the behavior of the polycation. These observations were further proven by  $\zeta$ -potential measurements (Figure 1D), revealing an overall negative charge until a pH of around 3, before positive values are obtained at pH 2.

While a clear increase of the  $T_{\text{CP}}$  from 28 to 40 °C from pH 5 to 1 is observed for PDha-g-NIPAAm<sub>50</sub> (36 wt% NIPAAm, Figure 1D), in case of PDha-g-NIPAAm<sub>95</sub> (55 wt% NIPAAm),

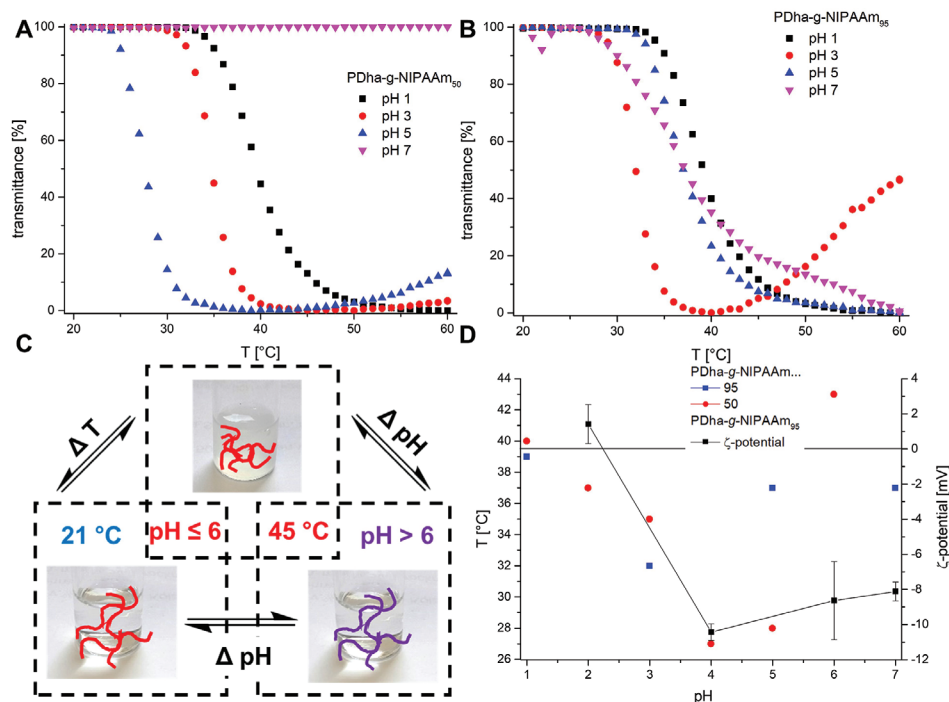


**Figure 1.** A,B) Cloud points determined from UV–vis measurements of PDha-g-NIPAAm<sub>95</sub> and PDha-g-NIPAAm<sub>50</sub> at different pH values ( $c = 1 \text{ mg mL}^{-1}$ , rate  $0.2 \text{ }^\circ\text{C min}^{-1}$ ). C) Schematic illustration of the on/off switching of the thermoresponsive behavior of PDha-g-NIPAAm<sub>50</sub> by changes in pH value. D) Diagram of  $T_{\text{CP}}$  versus pH value and  $\zeta$ -potential of PDha-g-NIPAAm<sub>95</sub>.

less variation is observed and the observed  $T_{CP}$  values are closer to those reported for the PNIPAAm homopolymer with a  $T_{CP}$  of 30–35 °C.<sup>[33]</sup> Exemplarily, at pH 1 we investigated the reversible aggregation of PDha-g-NIPAAm<sub>95</sub> by temperature-dependent <sup>1</sup>H-NMR spectroscopy and dynamic light scattering (DLS) measurements (Figure S4, Supporting Information). Regarding <sup>1</sup>H-NMR, the integrals of the –CH<sub>2</sub>– backbone at 2.17–2.84 ppm and (–CH<sub>3</sub>)<sub>2</sub> NIPAAm protons (0.84–1.14 ppm) decrease in intensity starting from 35 °C, as a result of the collapse of the graft copolymer. Upon cooling, a stepwise increase in intensity hints toward swelling and dissolving of the aggregates being formed. These observations were supported by DLS measurements (Figure S4B, Supporting Information), where first individual polymer chains were detected, and starting from 27 °C, aggregates with a hydrodynamic radius ( $R_H$ ) of 310 nm were found, further increasing in size up to 820 nm at 50 °C.

As a first and simple example of sensing, the  $T_{CP}$  can be used to monitor changes in local pH, as it is schematically shown in Figure 1C. At first, a solution of PDha-g-NIPAAm<sub>50</sub> (pH ≈ 7) was heated to 45 °C, where no  $T_{CP}$  was observed. After

addition of 0.1 M HCl so that a pH of ≤6 was reached, the solution became turbid, indicating LCST behavior. Upon returning to 21 °C the solution became clear again, and increasing the pH by addition of 0.1 M NaOH led to similar behavior as observed initially. This reversible response to changes in pH within a moderately narrow and biologically relevant window renders such graft copolymers interesting materials for biomedical applications, e.g., in carrier systems.<sup>[36]</sup>

The PDha backbone offers strong binding sites for metal ions and can act as a template for the formation of noble metal nanoparticles.<sup>[32]</sup> Simultaneously, solubility is mediated by remaining backbone and NIPAAm side-chain functionalities, and we therefore used both PDha-g-NIPAAm<sub>50</sub> and PDha-g-NIPAAm<sub>95</sub> for the chelation of metal ions. Cu<sup>2+</sup> or Pb<sup>2+</sup> (0.01 mmol mL<sup>-1</sup>) was added until the graft copolymer solutions (pH 7) became slightly opaque, indicating chelation and aggregation. Independent of the DoF, spherical aggregates were formed (Figure 2) with a size of  $R_H$  = 11–60 nm according to DLS (Figure S5, Supporting Information) and this was confirmed by transmission electron microscopy (TEM).

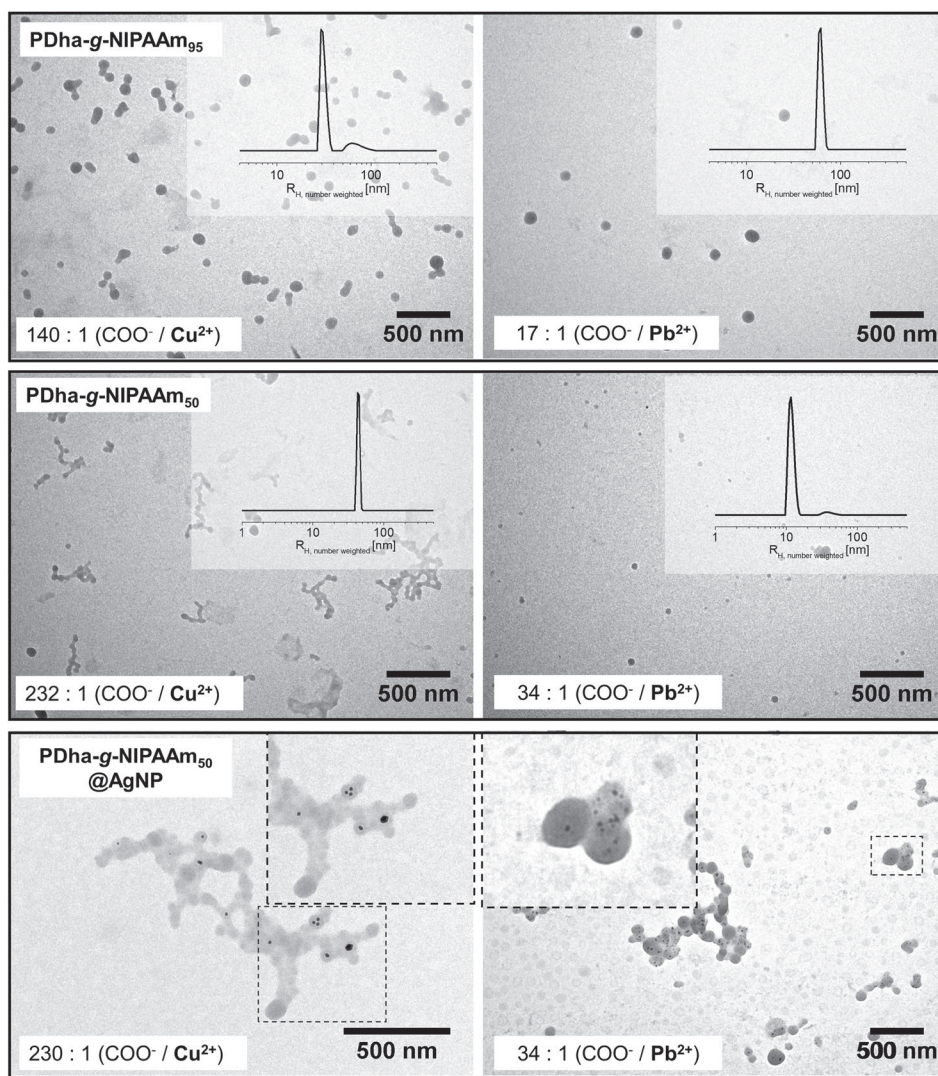


**Figure 2.** TEM micrographs of aggregates formed after addition of Cu<sup>2+</sup> and Pb<sup>2+</sup> to the graft copolymer solutions and AgNP dispersions.

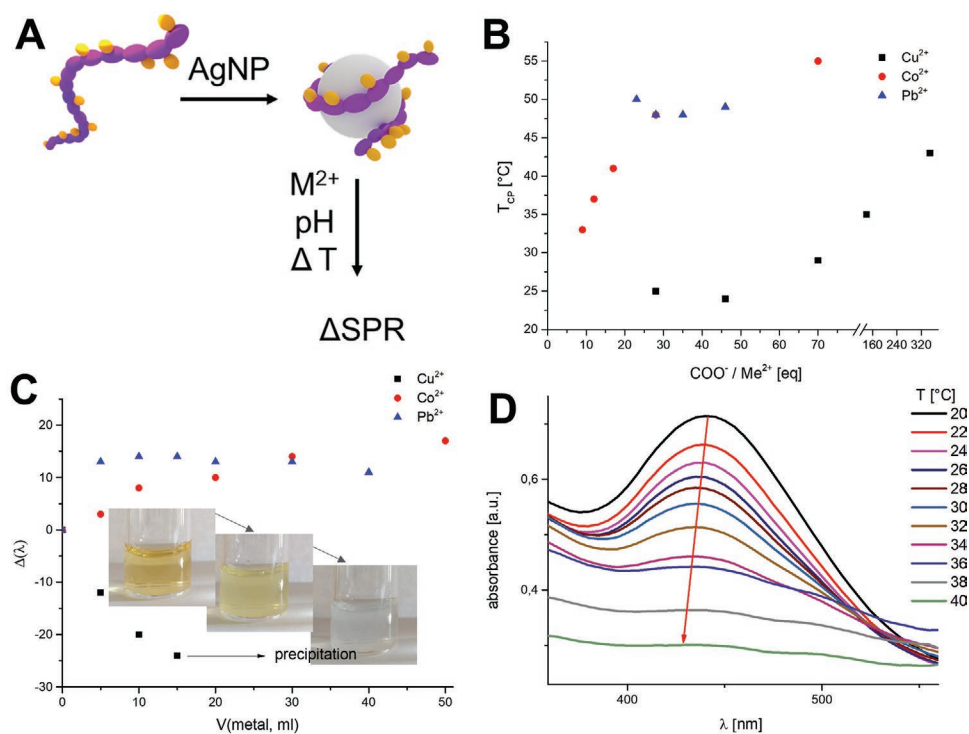


**Figure 3.** A) Formation of PDha-g-NIPAAm<sub>50</sub> and AgNP hybrid materials being responsive to metal cations, pH, and temperature changes. B)  $T_{CP}$  as a function of metals and their concentration after addition to PDha-g-NIPAAm<sub>50</sub>. C) Shift of the SPR wavelength maximum in presence of PDha-g-NIPAAm<sub>50</sub> as a function of metals and their concentration. D) The SPR is quenched when heated at pH 5 or lower.

We observed a high sensitivity toward the addition of  $Cu^{2+}$ , as already at a ratio of 1:230 ( $Cu^{2+}/COO^-$ ) visible aggregation occurred, while in case of  $Pb^{2+}$  ions, a higher amount of metal ions was necessary to induce the formation of aggregates (1:34). We tentatively ascribe this to different coordination behavior, in line with earlier studies on the complexation of different metal ions with poly(acrylamidoglycolic acid) (PAGA).<sup>[14]</sup> In addition, our results indicate that size and shape of the aggregates seem to depend on the type of metal ion and concentration, in accordance with literature examples,<sup>[13,14]</sup> as well as the DoF of NIPAAm side chains. We found that the morphology of PDha-g-NIPAAm in the presence of  $Pb^{2+}$  ions remains regularly spherical even though we vary both the PDha/NIPAAm and  $M^{2+}/PDha$  ratios. As these parameters show no significant influence on aggregate morphology, we hypothesize that the main driving force is the coordination behavior of  $Pb^{2+}$ . In the presence of  $Cu^{2+}$ , we have observed a morphological dependence mainly on the PDha/NIPAAm ratio. Multiple bridging of  $Cu^{2+}$  carboxylates is well known,<sup>[37]</sup> and this could lead to the formation of polymer aggregates and secondary aggregation at already low metal concentrations.

However, this, in our opinion, renders these graft copolymers even more applicable in sensing, using the hydrodynamic size and or measurable  $T_{CP}$  as signals for changes in pH or the presence of (traces of) metal ions. Complexation of the metal ions correlates also with inter- and intramolecular interactions and blocking of functional groups. As a result, thermoresponse was found for PDha-g-NIPAAm<sub>50</sub> even at pH 7, where previously aggregation was prevented by repulsive forces of the ionized moieties. We investigated the cloud points after  $Cu^{2+}$ ,  $Pb^{2+}$ , or  $Co^{2+}$  addition for different concentrations (Figure 3B)

and found distinct  $T_{CP}$ s. Except for  $Pb^{2+}$ ,  $T_{CP}$  is decreasing with higher metal concentrations that we attribute to an increased blocking of functional groups. Hereby, we found detection limits of 0.02, 0.15, and 0.1 mmol L<sup>-1</sup> for  $Cu^{2+}$ ,  $Pb^{2+}$ , and  $Co^{2+}$ , respectively. It is worth noting that these limits could be further adjusted by varying polymer concentration, DoF, or the pH value of the solution. Besides, other transition and main group metals could be recognized using the graft copolymer.

As an alternative readout signal, we exploited the ability of PDha-based materials to act as a template for the formation of noble metal nanoparticles and introduced silver nanoparticles (AgNPs) (Figure 3A), thereby imparting a strong surface plasmon resonance (SPR) signal within these hybrid materials. The SPR can then be used as an optical sensor responding to temperature, pH, and the presence of metal ions.<sup>[32,38,39]</sup> We were able to obtain AgNPs ( $R_H = 2.5$  nm from DLS) in the presence of PDha-g-NIPAAm<sub>50</sub> using  $NaBH_4$  as the reducing agent (Figure S6, Supporting Information). After addition of either  $Cu^{2+}$  or  $Pb^{2+}$ , the AgNPs were entrapped in the above-described aggregates, forming three-component nanomaterials as can be seen in TEM micrographs (Figure 2) and DLS (Figure S5, Supporting Information). As anticipated, a clear shift of the SPR peak was observed for PDha-g-NIPAAm<sub>50</sub>@AgNP core-shell nanomaterials upon complexation of metal ions (Figure 3C), resulting in a blueshift in case of  $Cu^{2+}$  ( $\Delta(\lambda)$  of up to 24 nm) and a redshift for  $Pb^{2+}$  and  $Co^{2+}$ . This process could be explained by either aggregation of AgNPs or decoration of the functional groups on the surface with the corresponding cations,<sup>[40]</sup> and this is also dependent on the metal concentration. Here, the detection limit was found to be 0.05 mmol L<sup>-1</sup> for each metal

tested. Being covered by a thermo- and pH-responsive shell, SPR of the AgNPs is further affected by the solution pH and temperature (Figures S7 and S8, Supporting Information). While the maximum SPR peak shifts by changing the pH value, it vanishes completely by heating due to aggregation at pH 5 and lower (Figure 3D; Figure S8 and Table S2, Supporting Information), further proving the concept of a multiresponsive graft copolymer and a sensitive detector for changes in pH, temperature, or the presence of metal ions.

In summary, we describe a facile strategy to obtain polyampholytic PDha-based triple-responsive graft copolymers. The materials feature tuneable output in terms of solubility or the SPR of immobilized AgNPs. Thereby, the measured output again depends on the amount of metal ion being present, the overall concentration, and the pH value of the medium. Although shown for AgNPs as a well-studied model system, the concept of using this graft copolymer as a template could be transferred to other metal NPs. In this regard, PDha-g-NIPAAm in our opinion is also an interesting starting point for soft-matter-based temperature-controlled catalysis.<sup>[41]</sup>

## Supporting Information

Supporting Information is available from the Wiley Online Library or from the author.

## Acknowledgements

This research was supported by the Deutsche Forschungsgemeinschaft (DFG, Project No. SCHA1640/18-1 and TRR234 “CataLight,” Project No. 364549901, project B5). The authors are grateful to Peggy Laudeley for SEC analysis and the NMR department at Friedrich-Schiller-University Jena for their continuous support. Further, the authors acknowledge the cryo-TEM/TEM facilities of the Jena Center for Soft Matter (JCSM), which were established with a grant from the German Research Council (DFG) and the European Funds for Regional Development (EFRE).

Open access funding enabled and organized by Projekt DEAL.

## Conflict of Interest

The authors declare no conflict of interest.

## Keywords

graft copolymers, metal sensors, polyampholyte, smart polymers, stimuli responsive materials

Received: November 9, 2020

Revised: November 27, 2020

Published online:

[1] L. A. Malik, A. Bashir, A. Qureshi, A. H. Pandith, *Environ. Chem. Lett.* **2019**, *17*, 1495.

[2] J. Hu, S. Liu, *Macromolecules* **2010**, *43*, 8315.

[3] M. Wei, Y. Gao, X. Li, M. J. Serpe, *Polym. Chem.* **2017**, *8*, 127.

[4] C. Pietsch, R. Hoogenboom, U. S. Schubert, *Angew. Chem., Int. Ed.* **2009**, *48*, 5653.

[5] Y. Chen, K.-Y. Pu, Q.-L. Fan, X.-Y. Qi, Y.-Q. Huang, X.-M. Lu, W. Huang, *J. Polym. Sci., Part A: Polym. Chem.* **2009**, *47*, 5057.

[6] Z. Guo, W. Zhu, H. Tian, *Macromolecules* **2010**, *43*, 739.

[7] T. Hosomi, H. Masai, T. Fujihara, Y. Tsuji, J. Terao, *Angew. Chem., Int. Ed.* **2016**, *55*, 13427.

[8] X. Liu, X. Zhou, X. Shu, J. Zhu, *Macromolecules* **2009**, *42*, 7634.

[9] M. Zhang, P. Lu, Y. Ma, J. Shen, *J. Phys. Chem. B* **2003**, *107*, 6535.

[10] P. Mi, L.-Y. Chu, X.-J. Ju, C. H. Niu, *Macromol. Rapid Commun.* **2008**, *29*, 27.

[11] J. Cheng, G. Shan, P. Pan, *Ind. Eng. Chem. Res.* **2017**, *56*, 1223.

[12] Q. Luo, Y. Guan, Y. Zhang, M. Siddiq, *J. Polym. Sci., Part A: Polym. Chem.* **2010**, *48*, 4120.

[13] A. Nabiyani, P. Biehl, F. H. Schacher, *Macromolecules* **2020**, *53*, 5056.

[14] L. Volkmann, M. Köhler, F. H. Sobotta, M. T. Enke, J. C. Brendel, F. H. Schacher, *Macromolecules* **2018**, *51*, 7284.

[15] M. Hess, R. G. Jones, J. Kahovec, T. Kitayama, P. Kratochvíl, P. Kubisa, W. Mormann, R. F. T. Stepto, D. Tabak, J. Vohlídal, E. S. Wilks, *Pure Appl. Chem.* **2006**, *78*, 2067.

[16] T. Zhu, Y. Sha, J. Yan, P. Pageni, M. A. Rahman, Y. Yan, C. Tang, *Nat. Commun.* **2018**, *9*, 4329.

[17] Y. Liu, K. Ogawa, K. S. Schanze, *J. Photochem. Photobiol., C* **2009**, *10*, 173.

[18] B. L. Rivas, E. Pereira, R. Cid, K. E. Geckeler, *J. Appl. Polym. Sci.* **2005**, *95*, 1091.

[19] G. Craciun, E. Manaila, D. Ighigeanu, *Polymers* **2019**, *11*, 234.

[20] T. Zheng, M. Zhu, M. Waqas, A. Umair, M. Zaheer, J. Yang, X. Duan, L. Li, *RSC Adv.* **2018**, *8*, 38818.

[21] E. A. Hassan, M. L. Hassan, C. N. Moorefield, G. R. Newkome, *Carbohydr. Polym.* **2015**, *116*, 2.

[22] Y. Morishima, T. Kobayashi, S.-i. Nozakura, *Polym. J.* **1989**, *21*, 267.

[23] F. Schacher, T. Rudolph, F. Wieberger, M. Ulbricht, A. H. E. Müller, *ACS Appl. Mater. Interfaces* **2009**, *1*, 1492.

[24] X. Zhang, K. Matyjaszewski, *Macromolecules* **1999**, *32*, 1763.

[25] C. Frangville, Y. Li, C. Billotey, D. R. Talham, J. Taleb, P. Roux, J.-D. Marty, C. Mingotaud, *Nano Lett.* **2016**, *16*, 4069.

[26] C. M. Schilli, M. Zhang, E. Rizzardo, S. H. Thang, Y. K. Chong, K. Edwards, G. Karlsson, A. H. E. Müller, *Macromolecules* **2004**, *37*, 7861.

[27] N. do Nascimento Marques, A. M. da Silva Maia, R. de Carvalho Balaban, *Polímeros* **2015**, *25*, 237.

[28] E. A. Bekturov, S. E. Kudaibergenov, S. R. Rafikov, *J. Macromol. Sci., Part C: Polym. Rev.* **1990**, *30*, 233.

[29] M. Billing, G. Festag, P. Bellstedt, F. H. Schacher, *Polym. Chem.* **2017**, *8*, 936.

[30] J. B. Max, D. V. Pergushov, L. V. Sigolaeva, F. H. Schacher, *Polym. Chem.* **2019**, *10*, 3006.

[31] J. B. Max, P. J. Mons, J. C. Tom, F. H. Schacher, *Macromol. Chem. Phys.* **2020**, *221*, 1900383.

[32] J. B. Max, K. Kowalczyk, M. Köhler, C. Neumann, F. Pielenz, L. V. Sigolaeva, D. V. Pergushov, A. Turchanin, F. Langenhorst, F. H. Schacher, *Macromolecules* **2020**, *53*, 4511.

[33] H. G. Schild, *Prog. Polym. Sci.* **1992**, *17*, 163.

[34] U. Günther, L. V. Sigolaeva, D. V. Pergushov, F. H. Schacher, *Macromol. Chem. Phys.* **2013**, *214*, 2202.

[35] S. Chen, K. Wang, W. Zhang, *Polym. Chem.* **2017**, *8*, 3090.

[36] Z. Ge, S. Liu, *Chem. Soc. Rev.* **2013**, *42*, 7289.

[37] J. Boonmak, S. Youngme, T. Chotkhun, C. Engkagul, N. Chaichit, G. A. van Albada, J. Reedijk, *Inorg. Chem. Commun.* **2008**, *11*, 1231.

[38] M. von der Lüche, U. Günther, A. Weidner, C. Gräfe, J. H. Clement, S. Dutz, F. H. Schacher, *RSC Adv.* **2015**, *5*, 31920.

[39] M. von der Lüche, A. Weidner, S. Dutz, F. H. Schacher, *ACS Appl. Nano Mater.* **2017**, *1*, 232.

[40] M. Annadhasan, T. Muthukumarasamyvel, V. R. Sankar Babu, N. Rajendiran, *ACS Sustainable Chem. Eng.* **2014**, *2*, 887.

[41] S. Carregal-Romero, N. J. Buurma, J. Pérez-Juste, L. M. Liz-Marzán, P. Hervés, *Chem. Mater.* **2010**, *22*, 3051.